World Applied Sciences Journal 16 (11): 1496-1508, 2012
ISSN 1818-4952

Monotone Data Visualization using Rational Functions

[1]*Malik Zawwar Hussain,* [2]*Muhammad Sarfraz,* [1]*Tahira Sumbal Shaikh*

[1]Department of Mathematics, University of the Punjab, Lahore, Pakistan
[2]Department of Information Science, Adailiya Campus, Kuwait University, Kuwait

Abstract: A piecewise rational cubic function is developed to preserve the shape of monotonic data. The rational cubic function has two free parameters in its description. Rational cubic functions are extended to rational bicubic partially blended functions. Simple data dependent constraints are derived on free parameters in the description of rational functions to conserve the shape of monotone 2D and 3D data. The developed schemes have unique representation. The error bounds of the piecewise rational cubic function is established as $O(h_i^3)$.

AMS subject classification 2000: 68U05 . 65D05 . 65D07 . 65D18

Key words: Data visualization . rational functions . interpolation . monotone data

INTRODUCTION

Data visualization is very important component of scientific research. It is a technique to convert data into visual display for gaining understanding and insight into the data. Data visualization has proved its importance in many areas including computer graphics, medical imaging, reverse engineering, architectural design, automotive, aerospace industries, earth and atmospheric science (geology, meteorology, oceanography and hydrology).

The data that is known may represent only a sample and may not be sufficient for physical interpretation of phenomenon of designer. To overcome this difficulty data is visualized in the form of curves and surfaces. It is required that visual model (curve or surface) must exhibit its inherent shape property to illustrate the meaning of scientific experiment. Monotone data arises in many physical process, engineering problems and scientific applications. To visualize the shape of the data such as ESR level in cancer patients and blood uric acid level in gout patients are examples of monotone curves. Non monotone visual models of these experiments misguide us about the health of the patient.

Smoothness is another significant requirement for the pleasing visual display of the data. If inherent shape properties of data are preserved but smoothness is not ensured then curves and surfaces will contain undesired oscillations. Cubic Hermite function schemes generate smooth curves and surfaces but are not helpful for the interpolation of the shaped data. Highly misguided results, violating the inherited features of the data, can be seen when visual models contain undesired wiggles and bumps as in Fig. 4 and 7.

In recent years, researchers [1-15] have spent considerable time in the field of data visualization and shape perservation. For instance, Asaturyan *et al*. [1] presented an automatic algorithm for the construction of local shape preserving interpolating splines. These splines satisfy the convexity and torsion criteria relative to the polygonal line connecting interpolation points. Casciola and Romani [2] discussed rational interpolants with tension parameters; they presented some rational interpolating techniques to reconstruct shape preserving bivariate NURBS. Duan *et al*. [4] discussed the error estimation of a rational cubic spline. Fritsch and Butland [6] presented a method for constructing local monotone piecewise cubic interpolation. Fritsch and Carlson [7] derived necessary and sufficient condition for a cubic function to be monotone on an interval where the degree of smoothness attained is C^1. Hussain and Sarfraz [9] discussed monotony of piecewise rational cubic interpolation by imposing constraints on free parameters. For this purpose, they introduced a C^1 piecewise rational cubic spline. Hussain and Maria [10] developed schemes for the visualization of monotone data. They, in their work, also attained the degree of smoothness as C^1. Sarfraz [15] also used a C^1 rational cubic spline for the visualization of 2D monotone data whereas Hyman [11] discussed monotony preservation using cubic interpolation. Sarfraz *et al*. [13] discussed the problem of positive 2D and 3D data.

Corresponding Author: Malik Zawwar Hussain, Department of Mathematics, University of the Punjab, Lahore, Pakistan

This paper is a continuation of contribution towards representing and visualizing the shaped data when it inherits monotone feature of shape. The shape preserving schemes, in the form of curves and surfaces, have been presented for monotone 2D and 3D data respectively. It is very important to mention here that the proposed schemes are different from their counter parts [9, 10, 13, 15] on the similar subject. It differs in various aspects including the followings:

- It introduces and develops a new piecewise rational cubic spline curve representation of the form cubic/quadratic and then extends it to its corresponding surface.
- It presents monotony of curves as well as surfaces.
- The newly proposed piecewise rational cubic spline curves have two free parameters in its piecewise representations which are further extended to their corresponding surfaces.
- Instead of calculating derivative parameters by arithmetic mean method, which usually does not work for monotone data, the derivative parameters are estimated by geometric mean method which is the appropriate estimator for the visualization of monotone data.
- The error bounds of the proposed piecewise rational cubic are established as $O(h_i^3)$.
- The proposed schemes reduce the higher order arithmetic into lower degree arithmetic and are local.

The proposed methods, in this paper, have also the following important and advantageous features:

- It produces C^1 interpolant.
- No additional points (knots) are needed.
- The curve interpolant is not concerned with an arbitrary degree, it is a rational cubic spline of the form cubic/quadratic, it reduces to a Hermite cubic in a special setting of shape parameters. Same features are true for the surface interpolant.
- Once, the shape parameters are selected, the curve and surface representationsare unique in its solutions.
- It provides a guaranteed and unique alternate solution.
- The proposed methodsare automated monotonic data preserving schemes.
- There is no restriction on the number of data points, the curve and surface schemes work for any number of data points.

This paper has been organized as follows. In Section 2, a rational cubic function is introduced with two free parameters in its description. Derivative approximation scheme is also introduced, in this section, together with error analysis of the rational cubic functions. In Section 3, a scheme is developed to visualize monotone data in the view of C^1 monotone curves by making constraints on free parameters. In Section 4, rational cubic function is extended to rational bicubic partially blended function. In Section 5, a scheme is presented to visualize 3D monotone data in the view of monotone surfaces. Section 6 concludes the paper.

RATIONAL CUBIC FUNCTION

In this section, a C^1 rational cubic function with two free parameters has been developed. Let $\{(x_i, f_i), i = 1,2,3,\ldots,n\}$ be given set of data points where $x_1<x_2<\ldots<x_n$. In each interval $I_i = [x_i, x_{i+1}]$, a rational cubic function $S_i(x)$ may define as:

$$S(x) \equiv S(x_i) = \frac{\mu_i U_i (1-\theta)^3 + W_i\theta(1-\theta)^2 + T_i\theta^2(1-\theta) + \upsilon_i V_i \theta^3}{\mu_i (1-\theta)^2 + (\mu_i + \upsilon_i)\,\theta(1-\theta) + \upsilon_i\theta^2} \quad (1)$$

with

$$U_i = f_i,\ W_i = \mu_i h_i d_i + (2\mu_i + \upsilon_i) f_i,$$

$$T_i = -\upsilon_i h_i d_{i+1} + (\mu_i + 2\upsilon_i) f_{i+1},\ V_i = f_{i+1},$$

$$h_i = x_{i+1} - x_i,\ \theta = (x - x_i)/h_i,\ i = 1,2,3,\ldots,n-1$$

Rational cubic function (1) has following interpolatory properties:

$$\left.\begin{array}{ll} S(x_i) = f_i, & S(x_{i+1}) = f_{i+1}, \\ S^{(1)}(x_i) = d_i, & S^{(1)}(x_{i+1}) = d_{i+1}, \end{array}\right\}$$

where $S^{(1)}(x_i)$ denotes derivative with respect to x and d_i denotes derivative value given or estimated by some approximate method at the knot x_i. In each interval $[x_i, x_{i+1}]$, the rational cubic function $S(x) \in C^1[x_1, x_n]$ has free parameters $\mu_i's$, and $\upsilon_i's$.

Remark 1: In each interval $[x_i, x_{i+1}]$, it can be noted that when $\mu_i = \upsilon_i = 1$, the rational cubic function (1) becomes the standard cubic Hermite function.

Determination of derivatives: It often happens that the derivative parameters $\{d_i's\}$ are not given and hence are needed to be determined by some suitable methods. In this work, they are computed from the geometric mean method. These are the non-linear approximations which are defined as follows:

$$d_i = \begin{cases} 0 & \text{if } \Delta_{i-1} = 0 \ \ \Delta_i = 0, \\ \Delta_{i-1}^{h_i/(h_{i-1}+h_i)} \Delta_i^{h_{i-1}/(h_{i-1}+h_i)} & \text{otherwise}, i = 1,2,\ldots,n-1 \end{cases}$$

$$d_1 = \begin{cases} 0 & \text{if } \Delta_1 = 0 \ \text{or} \ \Delta_{3,1} = 0 \\ \Delta_1 \left\{\Delta_1/\Delta_{3,1}\right\}^{h_1/h_2} & \text{otherwise} \end{cases}$$

$$d_n = \begin{cases} 0 & \text{if } \Delta_{n-1} = 0 \ \text{or} \Delta_{n,n-2} = 0 \\ \Delta_{n-1} \left\{\Delta_{n-1}/\Delta_{n,n-2}\right\}^{h_{n-1}/h_{n-2}} & \text{otherwise} \end{cases}$$

where

$$\Delta_{3,1} = (f_3 - f_1)/(x_3 - x_1), \ \Delta_{n,n-2} = (f_n - f_{n-2})/(x_n - x_{n-2})$$

Error estimation: In this section the error bound of the rational cubic function is estimated when the rational cubic function being interpolated is C^1. The interpolating scheme developed in Section 2 is local that allows to investigate the error bounds of rational cubic function in an arbitrary subinterval $I_i = [x_i, x_{i+1}]$ without loss of generality. Using Peano Kernel Theorem [5], the error of rational cubic function in each subinterval $I_i = [x_i, x_{i+1}]$ is as follows:

$$R[f] = f(x) - S(x) = \frac{1}{2}\int_{x_i}^{x_{i+1}} f^{(3)}(\tau) R_x\left[(x-\tau)_+^2\right] d\tau \qquad (2)$$

Considering the absolute value of Equation (2),

$$\left|f(x) - S(x)\right| = \left|\frac{1}{2}\int_{x_i}^{x_{i+1}} f^{(3)}(\tau) R_x\left[(x-\tau)_+^2\right] d\tau\right|$$

Using the uniform norm, the above equation takes the form:

$$\left|f(x) - S(x)\right| \le \frac{1}{2}\left\|f^{(3)}(\tau)\right\| \int_{x_i}^{x_{i+1}} \left|R_x\left[(x-\tau)_+^2\right]\right| d\tau,$$

where

$$R_x\left[(x-\tau)_+^2\right] = \begin{Bmatrix} \eta(\tau,x), & x_i < \tau < x \\ \xi(\tau,x), & x < \tau < x_{i+1} \end{Bmatrix}.$$

$R_x\left[(x-\tau)_+^2\right]$ is called Kernel of the integral in Equation (2). Also, the kernel functions $\eta(\tau,x)$ and $\xi(\tau,x)$, are presented as follows:

$$\eta(\tau,x) = (x-\tau)^2 - \frac{1}{q_i(\theta)}\left\{\theta^2(1-\theta)\left[(\mu_i + 2\upsilon_i)(x_{i+1}-\tau)^2 - 2\upsilon_i h_i (x_{i+1}-\tau)\right] + \upsilon_i (x_{i+1}-\tau)^2\theta^3\right\}$$

$$x_i < \tau < x$$

$$\xi(\tau,x) = -\frac{1}{q_i(\theta)}\left\{\theta^2(1-\theta)\left[(\mu_i + 2\upsilon_i)(x_{i+1}-\tau)^2 - 2\upsilon_i h_i (x_{i+1}-\tau)\right] + \upsilon_i (x_{i+1}-\tau)^2\theta^3\right\} \quad x < \tau < x_{i+1}$$

For error estimate representation, $\left|R[f]\right|$, we first discuss the properties of the kernel functions $\eta(\tau,x)$ and $\xi(\tau,x)$, then calculate the values of

$$\int_{x_i}^{x} \left|\eta(\tau,x)\right| d\tau \ \text{and} \ \int_{x}^{x_{i+1}} \left|\xi(\tau,x)\right| d\tau.$$

Part 1: Study the properties of the function $\eta(\tau,x)$. Consider $\eta(\tau,x)$, $\tau \in [x_i,x]$ as a function of τ, $\eta(\tau,x)$ is a quadratic polynomial of variable τ. According to the construction of kernel function $\eta(\tau,x)$ in using the Peano-Kernal theorem, $\forall\theta \in [0,1]$. It is observed that: $\eta(x_i,x) = 0$. Now, by substituting $\tau = x$ in $\eta(\tau,x)$ and after some simplifications, it becomes:

$$\eta(x,x) = -\frac{\theta^2(1-\theta)^2 h_i^2}{q_i(\theta)}\left\{\mu_i(1-\theta) - \upsilon_i\theta\right\}$$

Let $\mu_i(1-\theta)-\upsilon_i\theta = 0$ be considered in θ, its roots in (0,1) is

$$\theta^* = \frac{\mu_i}{\mu_i + \upsilon_i} \qquad (3)$$

It is easy to show that $\eta(x,x)\le 0$ for $\theta\le\theta^*$ and when $\theta\ge\theta^*$, we have $\eta(x,x)\ge 0$. To see the sign of $\eta(\tau,x)$ in $[x_i,x]$, rewrite $\eta(\tau,x)$ as:

$$\eta(\tau,x)=\frac{1}{q_i(\theta)}\Big[\Big((1+\theta)^2(1-\theta)^2\mu_i+\theta(1-\theta)^2\upsilon_i\Big)(x-\tau)^2-2\theta^2(1-\theta)^2h_i(\mu_i+\upsilon_i)(x-\tau)+\theta^2(1-\theta)^2h_i^2\big((\mu_i+\upsilon_i)\theta-\mu_i\big)\Big] \quad (4)$$

Then it can be found that second root of $\eta(\tau,x)$ is:

$$\tau^* = x-\frac{h_i\theta\big((\theta-1)\mu_i+\theta\upsilon_i\big)}{(1+\theta)\mu_i+\theta\upsilon_i}$$

beside the root $\tau^* = x_i$ and when $\theta>\theta^*$, we have $x_i<\tau^*<x$ and when $\theta<\theta^*$ we have $\tau^*>x$. Thus when $\theta<\theta^*$, $\eta(\tau,x)<0$ $\forall\tau\in[x_i,x]$, so

$$\int_{x_i}^{x}\big|\eta(\tau,x)\big|d\tau=\int_{x_i}^{x}\big(-\eta(\tau,x)\big)d\tau=\frac{\theta^3(1-\theta)^2\big((2-\theta)\mu_i-\theta\upsilon_i\big)h_i^3}{3\big((1-\theta)\mu_i+\upsilon_i\theta\big)} \quad (5)$$

When $\theta>\theta^*$, the values of $\eta(\tau,x)$ varr from negative to positive on the two sides of τ^*, so

$$\int_{x_i}^{x}\big|\eta(\tau,x)d\tau\big|=\int_{x_i}^{\tau^*}\big(-\eta(\tau,x)\big)d\tau+\int_{\tau^*}^{x}\big(\eta(\tau,x)\big)d\tau,$$

or

$$\int_{x_i}^{x}\big|\eta(\tau,x)d\tau\big|=\frac{1}{R}\Big\{\theta^3(1-\theta)^2\Big[\big((2-\theta)\mu_i-\theta\upsilon_i\big)\big((1+\theta)\mu_i+\theta\upsilon_i\big)^2+2\big((2+\theta)\mu_i+\theta\upsilon_i\big)\big((\theta-1)\mu_i+\theta\upsilon_i\big)^2\Big]h_i^3\Big\} \quad (6)$$

where

$$R=3\big((1-\theta)\mu_i+\upsilon_i\theta\big)\big((1+\theta)\mu_i+\upsilon_i\theta\big)^2$$

Part 2: Study the properties of $\xi(\tau,x)$. Consider $\xi(\tau,x)$, $\tau\in[x, x_{i+1}]$ as a function of τ, similar as discussed for $\eta(\tau,x)$. It is observed that $\xi(x_{i+1}, x) = 0$ and $\xi(x, x) = \eta(x, x)$ and by similar analysis as in Part 1, one can see that when $\theta\le\theta^*$, $\xi(x, x)\le 0$ and when $\theta\ge\theta^*$, $\xi(x, x)\ge 0$. To see the sign of $\xi(\tau,x)$ in $[x_i, x]$, rewrite $\xi(\tau,x)$ as:

$$\xi(\tau,x)=-\frac{(x_{i+1}-\tau)}{q_i(\theta)}\Big[\Big(\theta^2(1-\theta)^2\mu_i+\theta^2(2-\theta)\upsilon_i\Big)(x_{i+1}-\tau)-2\theta^2(1-\theta)\upsilon_ih_i\Big] \quad (7)$$

and denoting

$$\tau_*=x_{i+1}-\frac{2\theta^2(1-\theta)\upsilon_ih_i}{\theta^2(1-\theta)\mu_i+\theta^2(2-\theta)\upsilon_i}$$

It is easy to show that when $\theta\le\theta^*$ $\xi(\tau,x)$ varies from negative to positive on both sides of τ_* and when $\theta\ge\theta^*$, $\xi(\tau,x)$ remains positive in (x, x_{i+1}), where θ^* is defined as in (3). Thus when $\theta\le\theta^*$, we have:

$$\int_{x}^{x_{i+1}}\big|\xi(\tau,x)d\tau\big|=\int_{x}^{\tau_*}\big(-\xi(\tau,x)\big)d\tau+\int_{\tau_*}^{x_{i+1}}\xi(\tau,x)d\tau$$

or

$$\int_{x}^{x_{i+1}}\big|\xi(\tau,x)d\tau\big|=\frac{1}{R}\Big\{\theta^2(1-\theta)^3\Big[(1-\theta)^3(\mu_i+\upsilon_i)^3+3(\theta-1)\mu_i\upsilon_i^2+3\big((1+\theta)\upsilon_i^3\big)^2\Big]h_i^3\Big\} \quad (8)$$

where

$$R = 3\left((1-\theta)\mu_i + \upsilon_i\theta\right)\left((1+\theta)\mu_i + \upsilon_i\theta\right)^2$$

and when $\theta \geq \theta^*$

$$\int_{x}^{x_{i+1}} \left|\xi(\tau, x)\right| d\tau = \frac{\theta^2(1-\theta)^3\left((1+\theta)\upsilon_i - (1-\theta)\mu_i\right)h_i^3}{3\left((1-\theta)\mu_i + \upsilon_i\theta\right)} \tag{9}$$

Thus combining Equations (5) and (8), it can be shown that, when $\theta \leq \theta^*$

$$\left|f(x) - S(x)\right| \leq \frac{\left\|f^{(3)}\right\|}{2} \int_{x_i}^{x_{i+1}} \left|R_t\left[(x-\tau)_+^2\right]\right| d\tau = \left\|f^{(3)}\right\| h_i^3 \omega_1(\mu_i, \upsilon_i, \theta)$$

where

$$\omega_1(\mu_i, \upsilon_i, \theta) = \theta^2(1-\theta)^2\left[(1-\theta)^2\mu_i^3 + (1-\theta)(3-\theta)\mu_i^2\upsilon_i + \theta(2-\theta)\mu_i\upsilon_i^2 + \left(4 - 4\theta - \theta^2\right)\upsilon_i^3\right]\Big/ L \tag{10}$$

with

$$L = 6\left((1-\theta)\mu_i + \theta\upsilon_i\right)\left((1-\theta)\mu_i + (2-\theta)\upsilon_i\right)^2$$

Similarly, when $\theta \geq \theta^*$, combining the Equations (6) and (9), we have

$$\left|f(x) - S(x)\right| \leq \frac{\left\|f^{(3)}\right\|}{2} \int_{x_i}^{x_{i+1}} \left|R_x\left[(x-\tau)_+^2\right]\right| d\tau = \left\|f^{(3)}\right\| h_i^3 \omega_2(\mu_i, \upsilon_i, \theta)$$

where

$$\omega_2(\mu_i, \upsilon_i, \theta) = \theta^2(1-\theta)\left[\left(-\theta^2 + 6\theta - 1\right)\mu_i^3 + \left(1-\theta^2\right)\mu_i^2\upsilon_i + \theta(2+\theta)\mu_i\upsilon_i^2 + \theta^2\upsilon_i^3\right]\Big/ M \tag{11}$$

with

$$M = 6\left((1-\theta)\mu_i + \theta\upsilon_i\right)\left((1+\theta)\mu_i + \theta\upsilon_i\right)^2$$

Theorem 1: For $f(x) \in C^1[x_1, x_n]$, let S(x) be the rational cubic function *f*(x) in $[x_i, x_{i+1}]$ defined by Equation (1) for the positive parameter μ_i and υ_i, the error of the interpolating function S(x) satisfies

$$\left|f(x) - S(x)\right| \leq \left\|f^{(3)}\right\| h_i^3 c_i,$$

with $c_i = \max_{0 \leq \theta \leq 1} \omega(\mu_i, \upsilon_i, \theta)$, where

$$\omega(\mu_i, \upsilon_i, \theta) = \begin{cases} \omega_1(\mu_i, \upsilon_i, \theta), & 0 \leq \theta \leq \theta^* \\ \omega_2(\mu_i, \upsilon_i, \theta), & \theta^* \leq \theta \leq 1 \end{cases}$$

$\omega_1(\mu_i, \upsilon_i, \theta)$ and $\omega_2(\mu_i, \upsilon_i, \theta)$ are defined by Equations (10) and (11) respectively.

Remark 2: By taking $\mu_i = \upsilon_i = 1$, the rational cubic function defined in Equation (1) is the cubic Hermite function. In this case, the functions $\omega_1(\mu_i, \upsilon_i, \theta)$ and $\omega_2(\mu_i, \upsilon_i, \theta)$ become as follows:

$$\omega_1(\theta) = \frac{4\theta^2(1-\theta)^3}{3(3-2\theta)^2}, \quad 0 \leq \theta \leq \frac{1}{2}$$

$$\omega_2(\theta) = \frac{4\theta^3(1-\theta)^2}{3(1+2\theta)^2}, \quad \frac{1}{2} \leq \theta \leq 1.$$

Since

$$\max\left\{\max_{0 \leq \theta \leq \frac{1}{2}} \omega_1(\theta), \max_{\frac{1}{2} \leq \theta \leq 1} \omega_1(\theta)\right\} = \frac{1}{96}$$

It shows that the value of error coefficient is $c_i = \frac{1}{96}$. This is the well-known result for the standard cubic Hermite function.

Demonstration: In this section error of the rational cubic function is discussed numerically. For this, consider a function:

$$f(x) = \sqrt{x + 6.5} + (x + 2)^2, \quad \text{for } x \in [0, 16].$$

One can see the interpolating values of *f*(x) and S(x) are calculated at different knots x_i, as shown in

Table 1: The calculation for the function, spline and error

i	x_i	$f(x_i)$	$S(x_i)$	$\lvert S(x_i)-f(x_i)\rvert$
1	0.00	6.5495	6.5495	0.0000
2	0.20	7.4284	7.4279	0.0005
3	0.40	8.3868	8.3860	0.0008
4	0.60	9.4246	9.4235	0.0009
5	0.80	10.5419	10.5407	0.0009
6	1.00	11.7386	11.7375	0.0009
7	1.20	13.0149	13.0140	0.0009
8	1.40	14.3707	14.3700	0.0007
9	1.60	15.8060	15.8056	0.0004
10	1.80	17.3210	17.3207	0.0003
11	2.00	18.9155	18.9155	0.0000
12	2.20	20.5896	20.5898	0.0002
13	2.40	22.3433	22.3436	0.0009
14	2.60	24.1766	24.1770	0.0004
15	2.80	26.0896	26.0900	0.0004
16	3.00	28.0822	28.0825	0.0009
17	3.20	30.1545	30.1547	0.0002
18	3.40	32.3064	32.3065	0.0001
19	3.60	34.5380	34.5380	0.0000
20	3.80	36.8494	36.8493	0.0001
21	4.0	39.2404	39.2404	0.0000
22	4.20	41.7111	41.7112	0.0001
23	4.40	44.2615	44.2617	0.0002
24	4.60	46.8917	16.8919	0.0002
25	4.80	49.6015	49.6017	0.0002
26	5.0	52.3912	52.3913	0.0001
27	5.20	55.2605	55.2606	0.0001
28	5.40	58.2096	58.2096	0.0000
29	5.60	61.2385	61.2384	0.0001
30	5.80	64.3471	64.3471	0.0000
31	6.00	67.5355	67.5355	0.0000
32	6.20	70.8037	70.8037	0.0000
33	6.40	74.1517	74.1517	0.0000
34	6.60	77.5794	77.5795	0.0001
35	6.80	81.0869	81.0870	0.0001
36	7.00	84.6742	84.6734	0.0001
37	7.20	88.3414	88.3414	0.0000
38	7.40	92.0883	92.0883	0.0000
39	7.60	95.9150	95.9150	0.0000
40	7.80	99.8215	99.8215	0.0000
41	8.00	103.8079	103.8079	0.0000
42	8.20	107.8741	107.8741	0.0000
43	8.40	112.0201	112.0201	0.0000
44	8.60	116.2459	116.2460	0.0001
45	8.80	120.5515	120.5516	0.0001
46	9.00	124.9370	124.9371	0.0001
47	9.20	129.4023	129.4024	0.0001
48	9.40	133.9475	133.9475	0.0000

Table 1: Continued

i	x_i	$f(x_i)$	$S(x_i)$	$\lvert S(x_i)-f(x_i)\rvert$
49	9.60	138.5725	138.5724	0.0000
50	9.80	143.2773	143.2773	0.0000
51	10.00	148.0620	148.0620	0.0000
52	10.20	152.9266	152.9266	0.0000
53	10.40	157.8710	157.8710	0.0000
54	10.60	162.8952	162.8952	0.0000
55	10.80	167.9993	167.9993	0.0000
56	11.00	173.1833	173.1833	0.0000
57	11.20	178.4471	178.4471	0.0000
58	11.40	183.7908	183.7808	0.0000
59	11.60	189.2144	189.2143	0.0001
60	11.80	194.7178	194.7178	0.0000
61	12.00	200.3012	200.3011	0.0001
62	12.20	205.9643	205.9643	0.0000
63	12.40	211.7074	211.7074	0.0000
64	12.60	217.5304	217.5304	0.0000
65	12.80	223.4332	223.4332	0.0000
66	13.00	229.4159	229.4159	0.0000
67	13.20	235.4785	235.4785	0.0000
68	13.40	241.6209	241.6209	0.0000
69	13.60	127.8433	247.8433	0.0000
70	13.80	254.1456	254.1455	0.0001
71	14.00	260.5277	260.5277	0.0000
72	14.20	266.9897	266.9898	0.0001
73	14.40	273.5317	273.5317	0.0000
74	14.60	280.1535	280.1535	0.0000
75	14.80	286.8552	286.8552	0.0000
76	15.00	293.6368	293.6368	0.0000
77	15.20	300.4983	300.4983	0.0000
78	15.40	307.4397	307.4397	0.0000
79	15.60	314.4611	314.4610	0.0001
80	15.80	321.5623	321.5623	0.0000
81	16.00	238.7434	238.7434	0.0000

Table 1. Absolute error values of $f(x)$ and $S(x)$ are shown in column 5 of Table 1. It is clear from column 5 that up to three decimal places values of $f(x)$ and $S(x)$ is same. This shows that the order of the piecewise rational cubic function is $O(h_i^3)$.

Figure 1 is generated by the function $f(x) = \sqrt{x+6.5} + (x+2)^2$, for $x \in [0,16]$ and Fig. 2 is generated by the piecewise rational cubic function $S(x)$ developed in Section 2. Both Figures visually look same because error between $f(x)$ and $S(x)$ is very small. The insignificant error is demonstrated in Fig. 3.

MONOTONE RATIONAL CUBIC FUNCTION

Rational cubic function (1) has deficiencies to visualize the shape of monotone data. Some treatment

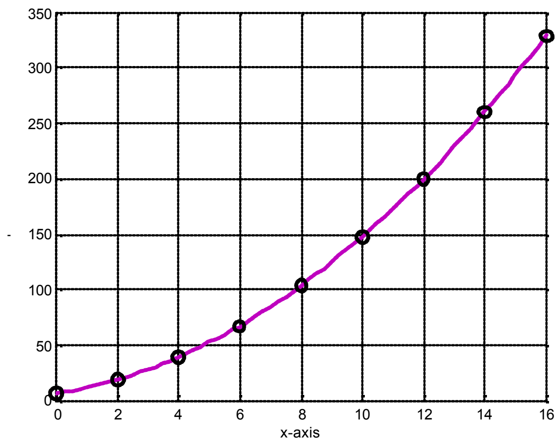

Fig. 1: Graph of the function f(x)

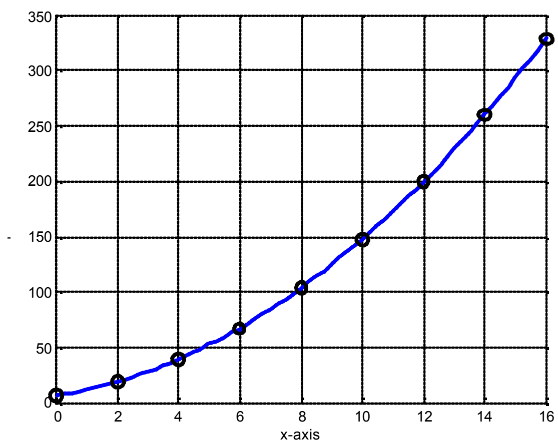

Fig. 2: Rational cubic spline

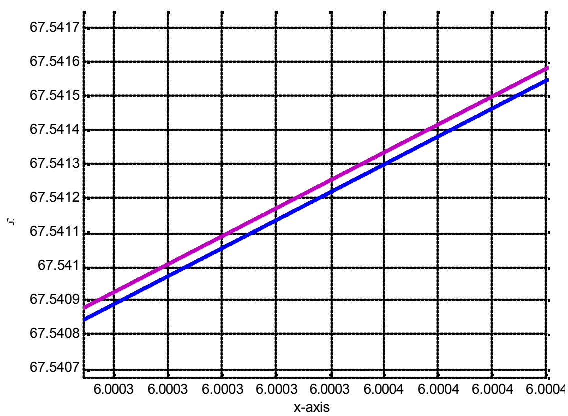

Fig. 3: Error between f(x) and S(x)

is required so that the visualization of monotone curve for the monotone data could be guaranteed. This leads towards some mathematical modeling by constraining some suitable automated values to the free parameters. This treatment is as follows:

Let $\{(x_i, f_i), i = 1,2,3,\ldots,n\}$ be a monotone set of data such that $x_1<x_2<\ldots x_n$ and $f_i \le f_{i+1}$,

$$\Delta_i = \frac{f_{i+1} - f_i}{h_i} \ge 0$$

$d_i \ge 0$, $i = 1,2,\ldots,n-1$. Now $S(x)$ is monotonically increasing if and only if $S^{(1)}(x) \ge 0$ for all $x \in [x_i, x_n]$. One can easily manipulate the following:

$$S^{(1)}(x) = \sum_{i=1}^{5} A_i \theta^{i-1} (1-\theta)^{5-i} \Big/ (q_i(\theta))^2 \tag{12}$$

where

$$A_1 = \mu_i^2 d_i$$

$$A_2 = 2\mu_i \upsilon_i (2\Delta_i - d_{i+1}) + 2\mu_i^2 \Delta_i$$

$$A_3 = \mu_i^2 (2\Delta_i - d_i) + 2\mu_i \upsilon_i \{4\Delta_i - d_{i+1} - d_i\} + \upsilon_i^2 (2\Delta_i - d_{i+1})$$

$$A_4 = 2\mu_i \upsilon_i (2\Delta_i - d_i) + 2\upsilon_i^2 \Delta_i$$

$$A_5 = \upsilon_i^2 d_{i+1}$$

Since the denominator in (12), being a squared quantity, is positive, therefore $S^{(1)}(x) \ge 0$ if $A_i^{'}s \ge 0$, $i = 1,2,\ldots,5$. It can be easily observed that $A_i^{'}s \ge 0$ if $\mu_i>0$, $\upsilon_i>0$, $\mu_i>d_i.\Delta_i$ and $\upsilon_i>d_{i+1}/\Delta_i$. Thus, all the above discussion is summarized in the following theorem:

Theorem 2: The rational cubic function (1) visualize the shape of monotone data in each interval $[x_i, x_{i+1}]$ if the free parameters satisfy the following conditions:

$$\mu_i = \alpha_i + d_i/\Delta_i, \alpha_i > 0$$

$$\upsilon_i = \beta_i + d_{i+1}/\Delta_i, \beta_i > 0$$

and all derivative parameters ’s are computed from the geometric means choice in Section 2.1.

Demonstration: This section is comprised with two practical examples to demonstrate the proposed curve scheme. In the first example, a monotone data is considered in Table 2. Figure 4 is drawn using cubic Hermite function form, it does not preserve the monotony. Figure 5 is fitted by using the monotone scheme developed in Section 3 which clearly conserves the monotony. Figure 6 is the merge of

Table 2: A monotone data

i	1	2	3	4	5
x_i	0	6	10	29.5	30
y_i	0.1	15	15	25	30

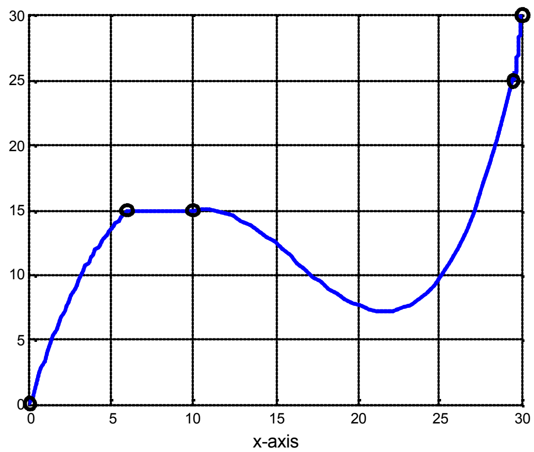

Fig. 4: Cubic hermite function

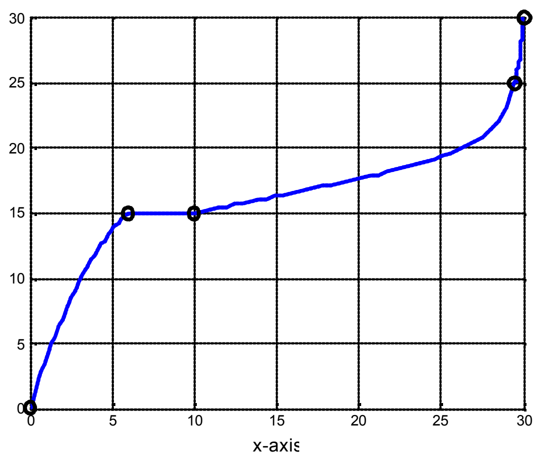

Fig. 5: C^1 monotone rational cubic function

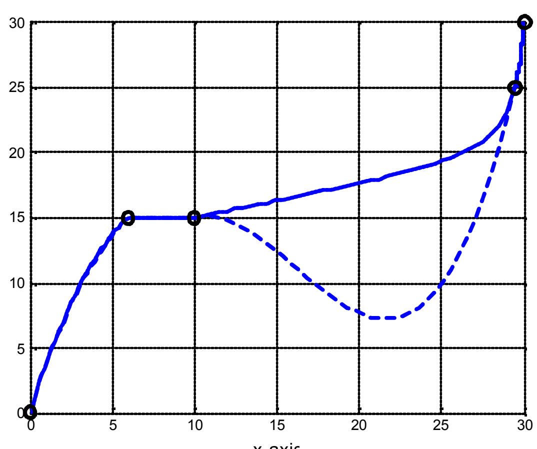

Fig. 6: Comparison between cubic hermite and C^1 function

Table 3: A monotone data

i	1	2	3	4	5
x_i	5	6	11	12	15
y_i	10	11	25	50	85

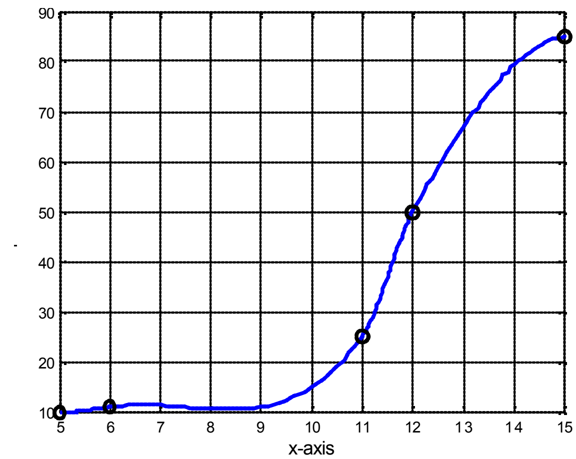

Fig. 7: Cubic hermite function

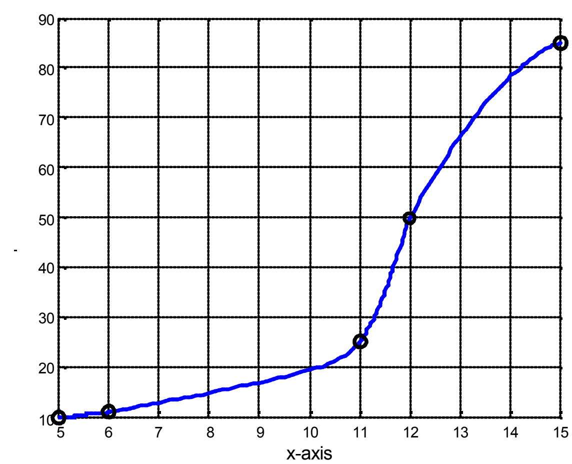

Fig. 8: C^1 monotone rational cubic function

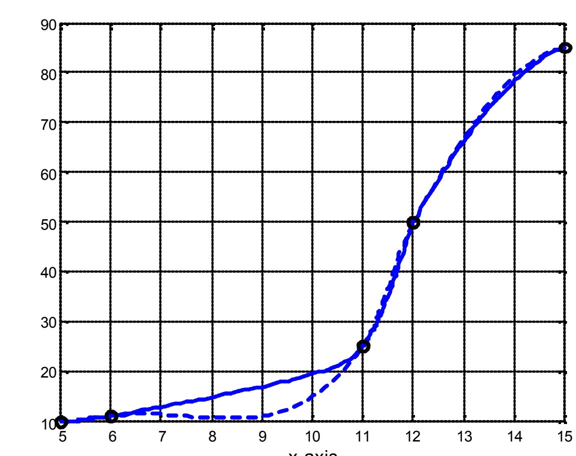

Fig. 9: Comparison between cubic Hermite and C^1 function

curves in Fig. 4 and 5 to see the clear difference of a simple cubic spline curve (dotted curve) and the proposed monotony preserving curve (solid curve) in one frame.

In the second example, another monotone data is considered in Table 3. Figure 7 is drawn using cubic Hermite function form, it does not preserve the monotony. Figure 8 is fitted by using the monotone scheme developed in Section 3 which clearly conserves the monotony. Figure 9 is the merge of curves in Fig. 7 and 8 to see the clear difference of a simple cubic spline curve (dotted curve) and the proposed monotony preserving curve (solid curve) in one frame.

RATIONAL BICUBIC FUNCTION

This section proposes an extension of the piecewise rational cubic function (1) to a rational bicubic partially blended function S(x,y) over the rectangular domain D = [a,b]×[c,d]. Let $\pi : a = x_1 < x_2 < \ldots < x_n = b$ be a partition of [a,b] and $\tilde{\pi} : c = y_1 < y_2 < \ldots < y_m = d$ be a partition of [c,d]. The rational bicubic partially blended function is defined over each rectangular patch $[x_i, x_{i+1}]\times[y_i, y_{i+1}]$, i = 1,2,…,n-1; j = 1,2,…,m-1 as:

$$S(x,y) = -AFB^T \tag{13}$$

where

$$F = \begin{pmatrix} 0 & S(x,y_j) & S(x,y_{j+1}) \\ S(x_i,y) & S(x_i,y_j) & S(x_i,y_{j+1}) \\ S(x_{i+1},y) & S(x_{i+1},y_j) & S(x_{i+1},y_{j+1}) \end{pmatrix}$$

$$A = \begin{bmatrix} -1 & a_0(\theta) & a_1(\theta) \end{bmatrix},\; B = \begin{bmatrix} -1 & b_0(\phi) & b_1(\phi) \end{bmatrix}$$

with

$$a_0 = (1-\theta)^2(1+2\theta),\; a_1 = \theta^3(3-2\theta)$$

$$b_0 = (1-\phi)^2(1+2\phi),\; b_1 = \phi^2(3-2\phi)$$

$$\theta = (x-x_i)/h_i,\; h_i = x_{i+1}-x_i, 0 \le \theta \le 1$$

$$\phi = (y-y_j)/\hat{h}_j, \hat{h}_j = y_{j+1}-y_j, 0 \le \phi \le 1$$

The functions $S(x,y_j)$, $S(x,y_{j+1})$, $S(x_i,y)$ and $S(x_{i+1},y)$ are same as rational cubic functions (1) defined over the boundary of rectangular patch $[x_i, x_{i+1}]\times[y_i, y_{i+1}]$. These are described in Equations (14-17) as:

$$S(x,y_j) = \sum_{i=1}^{4}(1-\theta)^{4-i}\theta^{i-1}A_{ij} \Big/ q_1(\theta) \tag{14}$$

with

$$A_{1j} = \mu_{i,j}^2 F_{i,j}$$

$$A_{2j} = (2\mu_{i,j}+\upsilon_{i,j})F_{i,j} + \mu_{i,j}h_i F_{i,j}^x$$

$$A_{3j} = (\mu_{i,j}+2\upsilon_{i,j})F_{i+1,j} - \upsilon_{i,j}h_i F_{i+1,j}^x$$

$$A_{4j} = \upsilon_{i,j}^2 F_{i+1,j}$$

$$q_1(\theta) = \mu_{i,j}(1-\theta)^2 + (\mu_{i,j}+\upsilon_{i,j})\theta(1-\theta) + \mu_{i,j}\theta^2$$

$$S(x,y_{j+1}) = \sum_{i=1}^{4}(1-\theta)^{4-i}\theta^{i-1}B_{ij} \Big/ q_2(\theta) \tag{15}$$

with

$$B_{1j} = \mu_{i,j+1}^2 F_{i,j+1}$$

$$B_{2j} = (2\mu_{i,j+1}+\upsilon_{i,j+1})F_{i,j+1} + \mu_{i,j+1}h_i F_{i,j+1}^x$$

$$B_{3j} = (\mu_{i,j+1}+2\upsilon_{i,j+1})F_{i+1,j+1} - \upsilon_{i,j+1}h_i F_{i+1,j+1}^x$$

$$B_{4j} = \upsilon_{i,j+1}^2 F_{i+1,j}$$

$$q_2(\theta) = \mu_{i,j+1}(1-\theta)^2 + (\mu_{i,j+1}+\upsilon_{i,j+1})\theta(1-\theta) + \mu_{i,j+1}\theta^2$$

$$S(x_i,y) = \sum_{i=1}^{4}(1-\phi)^{4-i}\phi^{i-1}C_{ij} \Big/ q_3(\phi) \tag{16}$$

with

$$C_{1j} = \hat{\mu}_{i,j}^2 F_{i,j}$$

$$C_{2j} = (2\hat{\mu}_{i,j}+\hat{\upsilon}_{i,j})F_{i,j} + \hat{\mu}_{i,j}\hat{h}_j F_{i,j}^y$$

$$C_{3j} = (\hat{\mu}_{i,j}+2\hat{\upsilon}_{i,j})F_{i,j+1} - \hat{\upsilon}_{i,j}\hat{h}_j F_{i,j+1}^y$$

$$C_{4j} = \hat{\upsilon}_{i,j}^2 F_{i,j+1}$$

$$q_3(\phi) = \hat{\mu}_{i,j}(1-\phi)^2 + (\hat{\mu}_{i,j}+\hat{\upsilon}_{i,j})\phi(1-\phi) + \hat{\mu}_{i,j}\phi^2$$

$$S(x_{i+1},y) = \sum_{i=1}^{4}(1-\phi)^{4-i}\phi^{i-1}D_{ij} \Big/ q_4(\phi) \tag{17}$$

with

$$D_{1j} = \hat{\mu}_{i+1,j}^2 F_{i,j}$$

$$D_{2j} = (2\hat{\mu}_{i+1,j}+\hat{\upsilon}_{i+1,j})F_{i+1,j} + \hat{\mu}_{i+1,j}\hat{h}_j F_{i+1,j}^y$$

$$D_{3j} = (\hat{\mu}_{i+1,j}+2\hat{\upsilon}_{i+1,j})F_{i+1,j+1} - \hat{\upsilon}_{i+1,j}\hat{h}_j F_{i+1,j+1}^y$$

$$D_{4j} = \hat{\upsilon}_{i+1,j}^2 F_{i+1,j+1}$$

$$q_4(\phi) = \hat{\mu}_{i+1,j}(1-\phi)^2 + (\hat{\mu}_{i+1,j}+\hat{\upsilon}_{i+1,j})\phi(1-\phi) + \hat{\mu}_{i+1,j}\phi^2$$

Remark 3: In each rectangular domain $[x_i, x_{i+1}]\times[y_i, y_{i+1}]$, it can be noted that when , the rational bicubic function (13) becomes the standard bicubic Hermite function.

Derivative for 3D data: It often happens that the derivative parameters are not given and hence are needed to be determined by some suitable methods. In this work, they are derived from the geometric mean method stated in Section 2.1. These are defined, for 3D data, as follows:

$$F^{x}_{i,j}=\begin{cases}0 & \text{if } \Delta_{i-1,j}=0 \text{ or } \Delta_{i,j}=0,\\ \Delta_{i-1,j}^{h_i/(h_{i-1}+h_i)}\Delta_{i,j}^{h_{i-1}/(h_{i-1}+h_i)} & \text{otherwise}, i=2,3,\ldots,n-1, j=1,2,\cdots,m\end{cases}$$

$$F^{x}_{1,j}=\begin{cases}0 & \text{if } \Delta_{1,j}=0 \text{ or } \Delta_{31,j}=0\\ \Delta_{1,j}\left\{\Delta_{1,j}/\Delta_{31,j}\right\}^{h_1/h_2} & \text{otherwise}\end{cases}$$

$$F^{x}_{n,j}=\begin{cases}0 & \text{if } \Delta_{n-1,j}=0 \text{ or } \Delta_{n(n-2),j}=0\\ \Delta_{n-1,j}\left\{\Delta_{n-1,j}/\Delta_{n(n-2),j}\right\}^{h_{n-1}/h_{n-2}} & \text{otherwise}\end{cases}$$

where

$$\Delta_{31,j}=(F_{3,j}-F_{1,j})/(x_3-x_1),\ \Delta_{n(n-2),j}=(F_{n,j}-F_{n-2,j})/(x_n-x_{n-2}), \Delta_{i,j}=\left(F_{i+1,j}-F_{i,j}\right)/h_i$$

Similarly

$$F^{y}_{i,j}=\begin{cases}0 & \text{if } \hat{\Delta}_{i,j-1}=0 \text{ or } \hat{\Delta}_{i,j}=0,\\ \hat{\Delta}_{i,j-1}^{\hat{h}_j/(\hat{h}_{j-1}+\hat{h}_j)}\hat{\Delta}_{i,j}^{\hat{h}_{j-1}/(\hat{h}_{j-1}+\hat{h}_j)} & \text{otherwise}, i=1,2,\ldots,n, j=2,3,\cdots,m-1\end{cases}$$

$$F^{y}_{i,1}=\begin{cases}0 & \text{if } \hat{\Delta}_{i,1}=0 \text{ or } \hat{\Delta}_{i,31}=0\\ \hat{\Delta}_{i,1}\left\{\hat{\Delta}_{i,1}/\hat{\Delta}_{i,31}\right\}^{\hat{h}_1/\hat{h}_2} & \text{otherwise}\end{cases}$$

$$F^{y}_{m,j}=\begin{cases}0 & \text{if } \hat{\Delta}_{i,m-1}=0 \text{ or } \hat{\Delta}_{i,m(m-2)}=0\\ \hat{\Delta}_{i,m-1}\left\{\hat{\Delta}_{i,m-1}/\hat{\Delta}_{i,m(m-2)}\right\}^{\hat{h}_{m-1}/\hat{h}_{m-2}} & \text{otherwise}\end{cases}$$

where

$$\hat{\Delta}_{i,31}=(F_{i,3}-F_{i,1})/(y_3-y_1),\ \hat{\Delta}_{i,m(m-2)}=(F_{i,m}-F_{i,m-2})/(y_m-y_{m-2}),\hat{\Delta}_{i,j}=\left(F_{i,j+1}-F_{i,j}\right)/\hat{h}_j$$

MONOTONE RATIONAL BICUBIC FUNCTION

Let

$$\left\{\left(x_i, y_j, F_{i,j}\right): i=1,2,\ldots n; j=1,2,\ldots m\right\}$$

be the given set of data points defined over rectangular grid

$$I_{i,j}=\left[x_i, x_{i+1}\right]\times\left[y_j, y_{j+1}\right]$$

$$i=1,2,\ldots,n-1; j=1,2,\ldots,m-1$$

the data will be monotone if it satisfy the following conditions:

$$F_{i,j}<F_{i,j+1},\ \Delta_{i,j}>0,\ F_{i,j}<F_{i+1,j},$$

$$\hat{\Delta}_{i,j}>0,\ F^{x}_{i,j}>0,\ F^{y}_{i,j}>0,\ \forall\, i,j$$

As in [2], bicubic partially blended surface patch inherits all the properties of network of boundary curves. Therefore, bicubic partially blended surface patch defined in (13) will be monotone in each rectangular patch $I_{i,j}=[x_i, x_{i+1}]\times[y_i, y_{i+1}]$, if each of the boundaries curve $S(x,y_j)$, $S(x,y_{j+1})$, $S(x_i,y)$ and $S(x_{i+1},y)$, is monotone. Thus, to prove the surface is monotony preserving, it is sufficient to show that

$$S^{(1)}\left(x,y_j\right)>0,\ S^{(1)}\left(x,y_{j+1}\right)>0,$$

$$S^{(1)}\left(x_i,y\right)>0,\ S^{(1)}\left(x_{i+1},y\right)>0,\ \forall\, i,j$$

Now

$$S^{(1)}\left(x,y_j\right)=\sum_{i=1}^{5}(1-\theta)^{5-i}\theta^{i-1}T_{ij}\Big/\left(q_1(\theta)\right)^2 \tag{18}$$

where

$$T_{1j} = \mu_{i,j}^2 F_{i,j}^x$$
$$T_{2j} = 2\mu_{i,j}\upsilon_{i,j}\left(2\Delta_{i,j} - F_{i+1,j}^x\right) + 2\mu_{i,j}^2\Delta_{i,j}$$
$$T_{3j} = \mu_{i,j}^2\left(2\Delta_{i,j} - F_{i,j}^x\right) + 2\mu_{i,j}\upsilon_{i,j}\left\{4\Delta_{i,j} - F_{i+1,j}^x - F_{i,j}^x\right\} + \upsilon_{i,j}^2\left(2\Delta_{i,j} - F_{i+1,j}^x\right)$$
$$T_{4j} = 2\mu_{i,j}\upsilon_{i,j}\left(2\Delta_{i,j} - F_{i,j}^x\right) + 2\upsilon_{i,j}^2\Delta_{i,j}$$
$$T_{5j} = \upsilon_{i,j}^2 F_{i+1,j}^x$$

Thus, $S^{(1)}(x,y_j)>0$, if $T_{i,j}>0$, $\forall i = 1,2,\ldots,5$. We can see that $T_{i,j}>0$ if

$$\mu_{i,j} > 0,\quad \upsilon_{i,j} > 0,\quad \mu_{i,j} > \frac{F_{i,j}^x}{\Delta_{i,j}},\quad \upsilon_{i,j} > \frac{F_{i+1,j}^x}{\Delta_{i,j}}$$

Similarly

$$S^{(1)}\left(x, y_{j+1}\right) = \sum_{i=1}^{5}(1-\theta)^{5-i}\theta^{i-1}S_{ij} \Big/ \left(q_2(\theta)\right)^2 \qquad (19)$$

where

$$S_{1j} = \mu_{i,j+1}^2 F_{i,j+1}^x$$
$$S_{2j} = 2\mu_{i,j+1}\upsilon_{i,j+1}\left(2\Delta_{i,j+1} - F_{i+1,j+1}^x\right) + 2\mu_{i,j+1}^2\Delta_{i,j+1}$$
$$S_{3j} = \mu_{i,j+1}^2\left(2\Delta_{i,j+1} - F_{i,j+1}^x\right) + 2\mu_{i,j+1}\upsilon_{i,j+1}\left\{4\Delta_{i,j+1} - F_{i+1,j+1}^x - F_{i,j+1}^x\right\} + \upsilon_{i,j+1}^2\left(2\Delta_{i,j+1} - F_{i+1,j+1}^x\right)$$
$$S_{4j} = 2\mu_{i,j+1}\upsilon_{i,j+1}\left(2\Delta_{i,j+1} - F_{i,j+1}^x\right) + 2\upsilon_{i,j+1}^2\Delta_{i,j+1}$$
$$S_{5j} = \upsilon_{i,j+1}^2 F_{i+1,j+1}^x$$

Thus, $S^{(1)}(x,y_{j+1})>0$, if $S_{i,j}>0$, $\forall i = 1,2,\ldots,5$. We can see that $S_{i,j}>0$, if

$$\mu_{i,j+1} > 0,\quad \upsilon_{i,j+1} > 0,\quad \mu_{i,j+1} > \frac{F_{i,j+1}^x}{\Delta_{i,j+1}},\quad \upsilon_{i,j+1} > \frac{F_{i+1,j+1}^x}{\Delta_{i,j+1}}$$

Similarly

$$S^{(1)}\left(x_i, y\right) = \sum_{i=1}^{5}(1-\phi)^{5-i}\phi^{i-1}U_{ij} \Big/ \hat{h}_j\left(q_3(\phi)\right)^2 \qquad (20)$$

where

$$U_{1j} = \hat{\mu}_{i,j}^2 F_{i,j}^y$$
$$U_{2j} = 2\hat{\mu}_{i,j}\hat{\upsilon}_{i,j}\left(2\hat{\Delta}_{i,j} - F_{i,j+1}^y\right) + 2\hat{\mu}_{i,j}^2\hat{\Delta}_{i,j}$$
$$U_{3j} = \hat{\mu}_{i,j}^2\left(2\hat{\Delta}_{i,j} - F_{i,j}^y\right) + 2\hat{\mu}_{i,j}\hat{\upsilon}_{i,j}\left\{4\hat{\Delta}_{i,j} - F_{i,j+1}^y - F_{i,j}^y\right\} + \hat{\upsilon}_{i,j}^2\left(2\hat{\Delta}_{i,j} - F_{i,j+1}^y\right)$$
$$U_{4j} = 2\hat{\mu}_{i,j}\hat{\upsilon}_{i,j}\left(2\hat{\Delta}_{i,j} - F_{i,j}^y\right) + 2\hat{\upsilon}_{i,j}^2\hat{\Delta}_{i,j}$$
$$U_{5j} = \hat{\upsilon}_{i,j}^2 F_{i,j+1}^y$$

Thus, $S^{(1)}(x_i,y)>0$, if $U_j>0$, $\forall i = 1,2,\ldots,5$. We can see that $U_{i,j}>0$, if

$$\hat{\mu}_{i,j} > 0,\quad \hat{\upsilon}_{i,j} > 0,\quad \hat{\mu}_{i,j} > \frac{F_{i,j}^y}{\hat{\Delta}_{i,j}},\quad \hat{\upsilon}_{i,j} > \frac{F_{i,j+1}^y}{\hat{\Delta}_{i,j}}$$

Similarly

$$S^{(1)}\left(x_{i+1}, y\right) = \sum_{i=1}^{5}(1-\phi)^{5-i}\phi^{i-1}W_{ij} \Big/ \hat{h}_j\left(q_4(\phi)\right)^2 \qquad (21)$$

where

$$W_{1j} = \hat{\mu}_{i+1,j}^2 F_{i+1,j}^y$$
$$W_{2j} = 2\hat{\mu}_{i+1,j}\hat{\upsilon}_{i+1,j}\left(2\hat{\Delta}_{i,j} - F_{i+1,j+1}^y\right) + 2\hat{\mu}_{i+1,j}^2\hat{\Delta}_{i,j}$$
$$W_{3j} = \hat{\mu}_{i+1,j}^2\left(2\hat{\Delta}_{i,j} - F_{i+1,j}^y\right) + 2\hat{\mu}_{i+1,j}\hat{\upsilon}_{i+1,j}\left\{4\hat{\Delta}_{i,j} - F_{i+1,j+1}^y - F_{i+1,j}^y\right\} + \hat{\upsilon}_{i+1,j}^2\left(2\hat{\Delta}_{i,j} - F_{i+1,j+1}^y\right)$$
$$W_{4j} = 2\hat{\mu}_{i+1,j}\hat{\upsilon}_{i+1,j}\left(2\hat{\Delta}_{i,j} - F_{i+1,j}^y\right) + 2\hat{\upsilon}_{i+1,j}^2\hat{\Delta}_{i,j}$$
$$W_{5j} = \hat{\upsilon}_{i+1,j}^2 F_{i+1,j+1}^y$$

Thus, $S^{(1)}(x_{i+1},y)>0$, if $W_{i,j}0$, $\forall i = 1,2,\ldots,5$. We can see that $W_{i,j}>0$, if

$$\hat{\mu}_{i+1,j} > 0,\quad \hat{\upsilon}_{i+1,j} > 0,\quad \hat{\mu}_{i+1,j} > \frac{F_{i+1,j}^y}{\hat{\Delta}_{i+1,j}},\quad \hat{\upsilon}_{i+1,j} > \frac{F_{i+1,j+1}^y}{\hat{\Delta}_{i+1,j}}$$

All this discussion is summarized in the following theorem:

Theorem 3: The rational bicubic partially blended functions defined in (13) visualize the shape of monotone data in each rectangular patch

$$I_{i,j} = \left[x_i, x_{i+1}\right] \times \left[y_j, y_{j+1}\right]$$

if the free parameters $\mu_{i,j}$, $\upsilon_{i,j}$, $\mu_{i,j+1}$, $\upsilon_{i,j+1}$, $\hat{\mu}_{i,j}$, $\hat{\upsilon}_{i,j}$, $\hat{\mu}_{i+1,j}$ and $\hat{\upsilon}_{i+1,j}$ satisfy the following conditions:

$$\mu_{i,j} = a_{i,j} + \frac{F_{i,j}^x}{\Delta_{i,j}},\qquad a_{i,j} > 0$$

$$\upsilon_{i,j} = b_{i,j} + \frac{F_{i+1,j}^x}{\Delta_{i,j}},\qquad b_{i,j} > 0$$

$$\mu_{i,j+1} = c_{i,j} + \frac{F_{i,j+1}^x}{\Delta_{i,j+1}},\quad c_{i,j} > 0$$

$$\upsilon_{i,j+1} = d_{i,j} + \frac{F_{i+1,j+1}^x}{\Delta_{i,j+1}},\ d_{i,j} > 0$$

Table 4: A 3D monotone data

y_i/x_i	-3	-2	-1	1	2	3
-3	-54	-35	-28	-26	-19	0
-2	-35	-16	-9	-7	0	19
-1	-28	-9	-2	0	7	26
1	-26	-7	0	2	9	28
2	-19	0	7	9	16	35
3	0	19	26	28	35	54

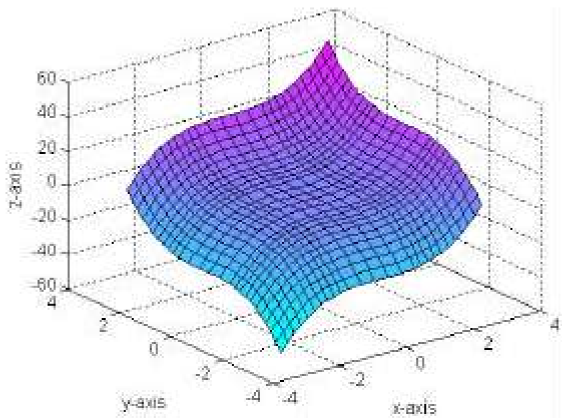

Fig. 10: Monotone rational bicubic function

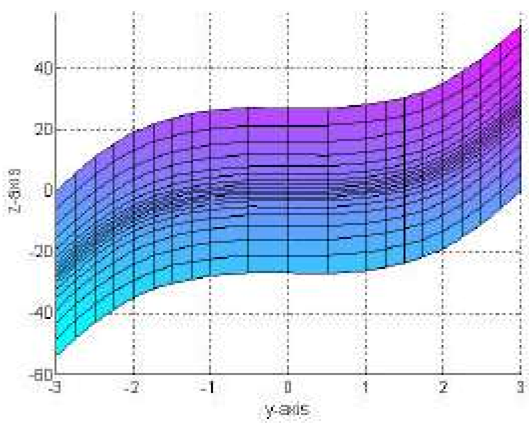

Fig. 11: yz-view of Fig. 10

$$\hat{\mu}_{i,j} = e_{i,j} + \frac{F^{y}_{i,j}}{\hat{\Delta}_{i,j}}, \qquad e_{i,j} > 0$$

$$\hat{\upsilon}_{i,j} = f_{i,j} + \frac{F^{y}_{i,j+1}}{\hat{\Delta}_{i,j}}, \quad f_{i,j} > 0$$

$$\hat{\mu}_{i+1,j} = g_{i,j} + \frac{F^{y}_{i+1,j}}{\hat{\Delta}_{i+1,j}}, \ g_{i,j} > 0$$

$$\hat{\upsilon}_{i+1,j} = h_{i,j} + \frac{F^{y}_{i+1,j+1}}{\hat{\Delta}_{i+1,j}}, h_{i,j} > 0$$

and derivative parameters are computed from the choice explained in Section 4.1.

Table 5: A 3D monotone data

y_i/x_i	1	2	3	4	5	6
1	0	1	10	33	76	145
2	10	32	98	232	458	800
3	34	91	252	571	1102	1899
4	78	184	478	1056	2014	3448
5	148	317	782	1693	3200	5453
6	250	496	1170	2488	4666	7920

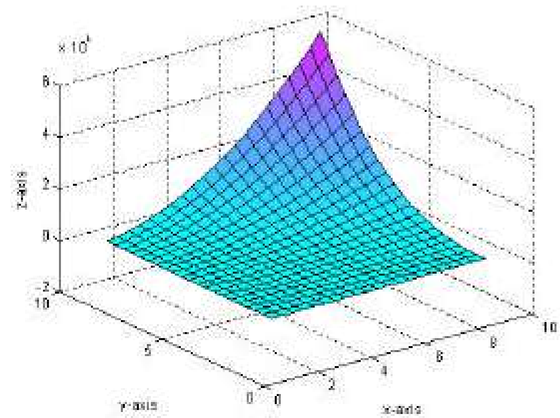

Fig. 12: Monotone rational bicubic function

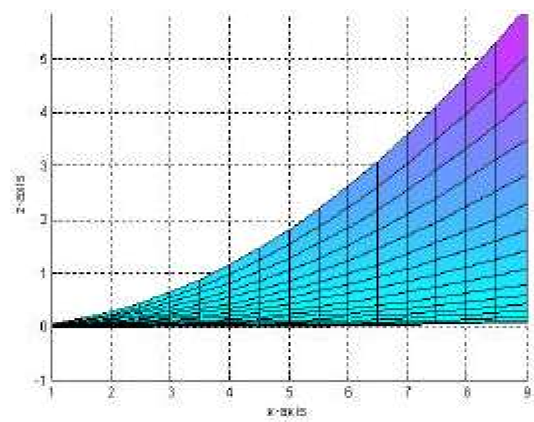

Fig. 13: xz-view of Fig. 12

Demonstration: This section demonstrates two examples of 3D monotone data to illustrate the proposed scheme. The first example is the monotone data set in Table 4 which is generated from the following monotonic function $F_1(x,y) = x^3+y^3$. The monotone surface, in Figure 10, is generated by Theorem 3 for the monotonic data in Table 4 with the choices: $a_{i,j} = 0.2$, $b_{i,j} = 0.2$, $c_{i,j} = 0.25$, $d_{i,j} = 0.25$, $e_{i,j} = 0.25$, $f_{i,j} = 0.25$, $g_{i,j} = 0.2$ and $h_{i,j} = 0.2$. Figure 11 shows the yz-view of Figure 10.

Another example is taken for a monotone data set in Table 5 which is generated from the following function:

$$F_2(x,y) = x^3 + x^2y^3 - 2y^2$$

The monotone surface, in Figure 12, is generated by the Theorem 3 for the monotonic data in Table 5 with the choices: $a_{i,j}$ = 0.25, $b_{i,j}$ = 0.25, $c_{i,j}$ = 0.2, $d_{i,j}$ = 0.2, $e_{i,j}$ = 0.2, $f_{i,j}$ = 0.2, $g_{i,j}$ = 0.25 and $h_{i,j}$ = 0.25. Figure 13 shows the xz-view of Figure 12.

CONCLUSION

A new C^1 rational cubic spline has been proposed together with the error analysis investigated of order $O(h_i^3)$. The proposed spline has been developed to visualize the C^1 monotone curves for the monotonic data. The C^1 monotone rational cubic spline has then been extended to monotone rational bicubic partially blended surfaces. Simple data dependent constraints are derived on the free parameters in the description of rational cubic functions and rational bicubic functions to ensure the shape of the data is preserved. The developed schemes are implemented on monotone data to visually demonstrate of the results.

REFERENCES

1. Asaturyan, S., P. Constantini and C. Manni, 2001. Local shape preserving interpolation by space curves. IMA Journal of Numerical Analysis, 21: 301-325.
2. Casciola, G. and L. Romani, 2003. Rational interpolants with tension parameters: Tom Lyche, Marie-Laurence Mazure and Larry L. Schumaker (Eds.). Curve and Surface Design, Nashboro Press, Brentwood, TN, pp: 41-50.
3. Duan, Q., X. Liu and F. Bao, 2008. Local shape control of the rational interpolation curves. International Journal of Computer Mathematics, 87 (3): 541-551.
4. Duan, Q., H. Zhang, Y. Zhang and E.H. Twizell, 2007. Error estimation of a kind of rational spline. Journal of Computational and Applied Mathematics, 200: 1-11.
5. Fangxun, B., S. Qinghua and Q. Duan, 2009. Point control of the interpolating curve with a rational cubic spline. Journal of Visual Commutation and Image Representation, 20: 275-280.
6. Fritsch, F.N. and J. Butland, 1984. A method for constructing local monotone piecewise cubic interpolation. SIAM Journal of Scientific and Statistical Computation, 5: 303-304.
7. Fritsch, F.N. and R.E Carlson, 1980. Monotone piecewise cubic interpolation. SIAM Journal of Numerical Analysis, 17 (2): 238-246.
8. Hussain, M.Z., M. Sarfraz and Maria Hussain, 2010. Scientific data Visualization with Shape Preserving C^1 rational cubic interpolation. European Journal of Pure and Applied Mathematics, 3 (2): 194-212.
9. Hussain, M.Z. and M. Sarfraz, 2009. Monotone piecewise rational cubic interpolation. International Journal of Computer Mathematics, 86 (3): 423-430.
10. Hussain, M.Z. and Maria Hussain, 2007. Visualization of data preserving monotonicity. Applied Mathematics and Computation, 190: 1353-1364.
11. Hyman, J.M., 1983. Accurate monotonicity preserving cubic interpolation. SIAM Journal of Scientific and Statistical Computation, 4 (4): 645-654.
12. Kouibia, A. and M. Pasadas, 2008. Approximation by interpolating variational splines. Journal of Computational and Applied Mathematics, 218: 342-349.
13. Srafraz, M., M.Z. Hussain and Asfar Nisar, 2010. Positive data modeling using spline function. Applied Mathematics and Computation, 216: 2036-2049.
14. Sarfraz, M. and M.Z. Hussain, 2006. Data visualization using rational spline interpolation. Journal of Computational and Applied Mathematics, 189: 513-525.
15. Sarfraz, M., 2003. A rational cubic spline for the visualization of monotonic data: An alternate approach. Computers and Graphics, 27: 107-121.